Inorganic Chemistry

Article

pubs.acs.org/IC

Sugar–Metal Ion Interactions: The Complicated Coordination Structures of Cesium Ion with D-Ribose and *myo*-Inositol

Haijian Hu,[†,‡] Junhui Xue,[§,∥] Xiaodong Wen,[†] Weihong Li,[§] Chao Zhang,[‡] Limin Yang,*[,†] Yizhuang Xu,*[,§] Guozhong Zhao,[⊥] Xiaoxia Bu,[⊥] Kexin Liu,[†] Jia'er Chen,[†] and Jinguang Wu[§]

[†]State Key Laboratory of Nuclear Physics and Technology, Institute of Heavy Ion Physics, School of Physics, Peking University, Beijing 100871, People's Republic of China

[‡]First Affiliated Hospital, Medical School, Xi'an Jiaotong University, Xi'an 710061, People's Republic of China

[§]Beijing National Laboratory for Molecular Sciences, State Key Laboratory for Rare Earth Materials Chemistry and Applications, College of Chemistry and Molecular Engineering, Peking University, Beijing 100871, People's Republic of China

[∥]Department of Chemistry, Renmin University of China, Beijing 100872, People's Republic of China

[⊥]Department of Physics, Capital Normal University, Beijing 100037, People's Republic of China

Supporting Information

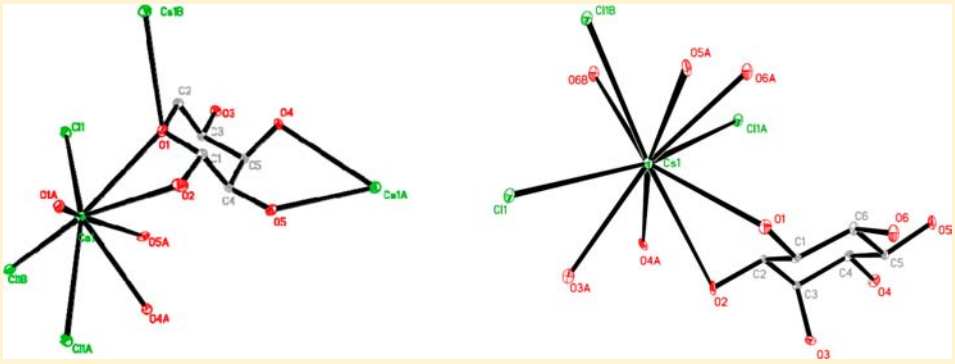

ABSTRACT: The novel cesium chloride–D-ribose complex ($CsCl{\cdot}C_5H_{10}O_5$; Cs-R) and cesium chloride–*myo*-inositol complex ($CsCl{\cdot}C_6H_{12}O_6$; Cs-I) have been synthesized and characterized using X-ray diffraction and FTIR, FIR, THz, and Raman spectroscopy. Cs^+ is eight-coordinated to three chloride ions, O1 and O2 from one D-ribose molecule, O1 from another D-ribose molecule, and O4 and O5 from the third D-ribose molecule in Cs-R. For one D-ribose molecule, the oxygen atom O1 in the ring is coordinated to two cesium ions as an oxygen bridge, O2 is cocoordinated with O1 to one of the two cesium ions, and O4 and O5 are coordinated to the third cesium ion, respectively. O3 does not coordinate to metal ions and only takes part in forming hydrogen bonds. One chloride ion is connected to three cesium ions. Thus, a complicated structure of Cs–D-ribose forms. For Cs-I, Cs^+ is 10-coordinated to three chloride ions, O1 and O2 from one *myo*-inositol molecule, O3 and O4 from another *myo*-inositol molecule, O5 and O6 from the third *myo*-inositol molecule, and O6 from the fourth *myo*-inositol molecule. One metal ion is connected to four ligands, and one *myo*-inositol is coordinated to four Cs^+ ions, which is also a complicated coordination structure. Crystal structure results, FTIR, FIR, THz, and Raman spectra provide detailed information on the structure and coordination of hydroxyl groups to metal ions in the cesium chloride–D-ribose and cesium chloride–*myo*-inositol complexes.

INTRODUCTION

The interactions between metal ions and carbohydrates are involved in many important biochemical processes.[1−3] It has also been exploited in metal-catalyzed enantioselective synthesis, therapeutic agents, catalysts and diagnostic tracers, etc.[4−8] Different saccharides have various coordination modes and some conformations; for example, *ax-eq-ax* conformations usually are favored for metal ion coordination.[1] D-Ribose ($C_5H_{10}O_5$, denoted as R here) is an important part of nucleic acid, which can interact with metal ions. Ribose interaction and complex formation with metal ions in neutral solutions have been studied for a large number of ions, e.g. La^{3+}, Ce^{3+}, Pr^{3+}, Nd^{3+}, Sm^{3+}, Eu^{3+}, Gd^{3+}, Tb^{3+}, Ca^{2+}, Sr^{2+}, Ba^{2+}, Cu^{2+}, and Mn^{2+}, mainly using calorimetric methods or NMR spectroscopy.[9−13] The investigation of the interaction of alkali halides with D-ribose by ^1H and ^{13}C NMR spectroscopy shows that the anion has a significant role.[14] Interactions of aluminum(III) with the biologically relevant ligand D-ribose has been discussed at different pH values and the results indicate the existence of association between Al(III) and D-ribose, stabilization of the "association" complex through hydrogen bonding, and subsequent complexation through proton release.[15] The effect of sodium

Received: August 6, 2013
Published: October 31, 2013

   dx.doi.org/10.1021/ic402027j | *Inorg. Chem.* 2013, 52, 13132−13145

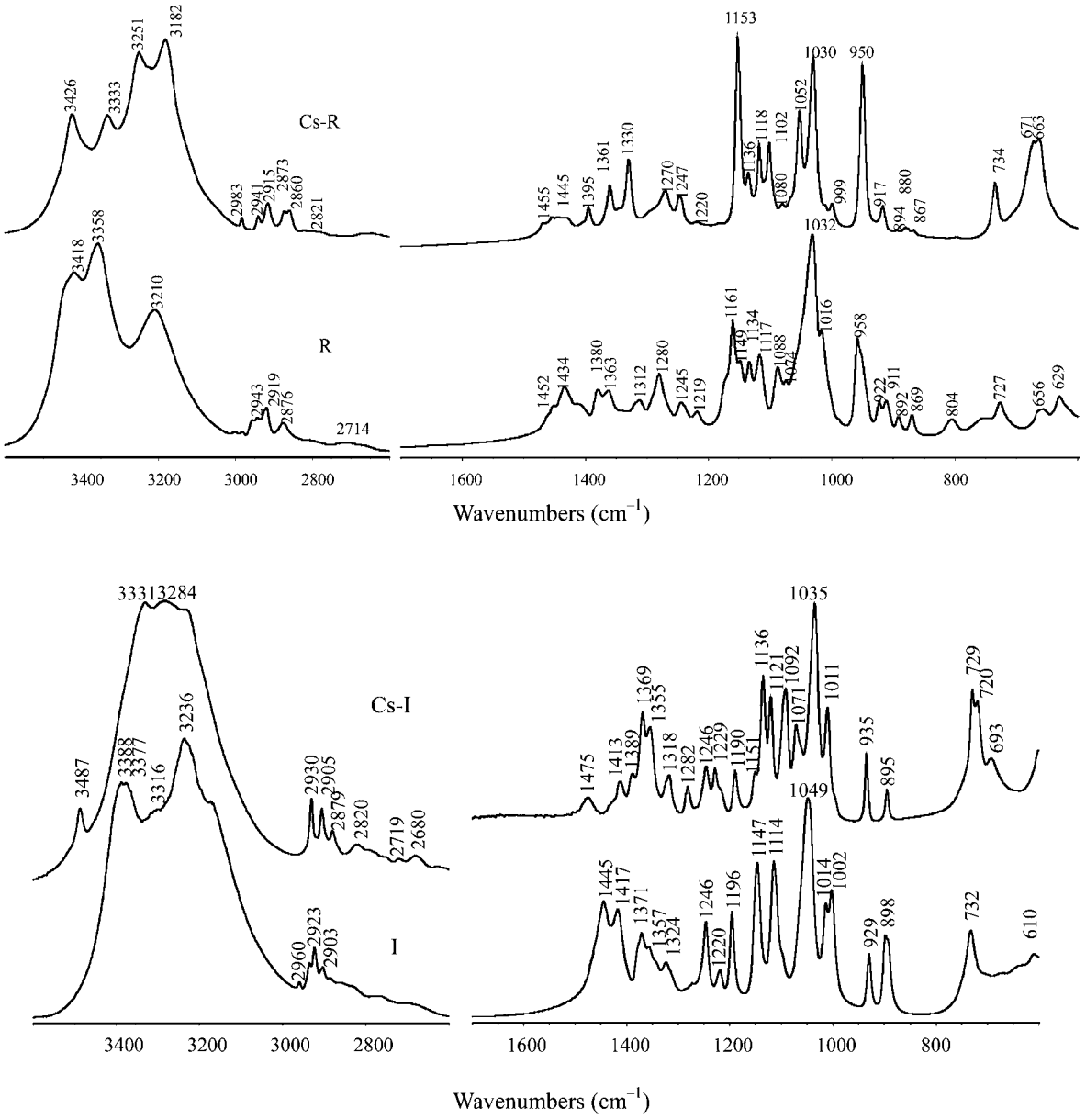

Figure 1. FTIR spectra of D-ribose, CsCl–D-ribose complex, *myo*-inositol, and CsCl–*myo*-inositol complex in the 3600–2600 and 1700–600 cm^{-1} regions.

acetate on the volumetric behavior of some mono-, di-, and trisaccharides in aqueous solutions over the temperature range 288.15–318.15 K is varied due to the interactions between solute (saccharide) and cosolute (sodium acetate).[16] Theoretical studies on the interaction between β-D-ribose and bivalent and monovalent cations have been carried out by Yang et al.[17] For *myo*-inositol, it binds with metal ions weakly in aqueous solution.[18−22] A trinuclear Cu(II) complex with inositol and 2,2′-bipyridine has been investigated as a hydrogelator for varied applications from superabsorbant materials to biosensors.[23]

In the solid state, for D-ribose, the single-crystal structures of its calcium and lanthanide complexes, including La^{3+}, Ce^{3+}, Pr^{3+}, Nd^{3+}, Sm^{3+}, and Eu^{3+} ions, have been reported,[24−32] in which D-ribose of a pyranose form is used as three hydroxyl donors in lanthanide complexes or D-ribose in a furanose form provides O1, O2, and O3 to one calcium ion and O4 and O5 to the second calcium ion. For deprotonated D-ribose, in the structure of its Pd complex $[(en)_2Pd_2(\beta\text{-D-Rib}p1,2,3,4H_{-4})]$) it acts as a bis-diolato ligand (O1 and O2 atoms are coordinated to one metal ion, and O3 and O4 atoms are coordinated to the second metal ion).[33] Rao et al. have reported the synthesis and characterization of some lanthanide– and transition-metal-ion–D-ribose complexes under alkaline conditions by various spectral and analytical techniques, and some appropriate structures have been assigned.[34,35] The crystal structures of metal–sugar complexes in a neutral state related to inositol, including $CaBr_2$·*myo*-inositol·$5H_2O$, $MgCl_2$·*myo*-inositol·$4H_2O$, $SrCl_2$·*epi*-inositol·$5H_2O$, $PrCl_3$·*myo*-inositol·$9H_2O$, and $NdCl_3$·*myo*-inositol·$9H_2O$ have been reported.[36−40] In these structures *myo*-inositol is coordinated to metal ions through pairs of adjacent hydroxyl groups (an axial–equatorial pair or an equatorial–equatorial pair). The crystal structures of $[V(H_{-3}\text{-}cis\text{-inositol})_2]$, $[K_2(cis\text{-inositol})_2]\cdot 4H_2O$, $[Na_6V(H_{-3}\text{-}cis\text{-inositol})_2](SO_4)_2\cdot 6H_2O$, and $K_5[OFe_6(cis\text{-inositol})_6H_{-21}]$ complexes formed in the alkaline state have been reported.[41,42] The authors also have demonstrated the coordination behavior of 1,3,5-triamino-1,3,5-trideoxy-*cis*-inositol (taci) and 1,3,5-trideoxy-1,3,5-tris(dimethylamino)-*cis*-inositol (tdci).[41] Most

dx.doi.org/10.1021/ic402027j | Inorg. Chem. 2013, 52, 13132−13145

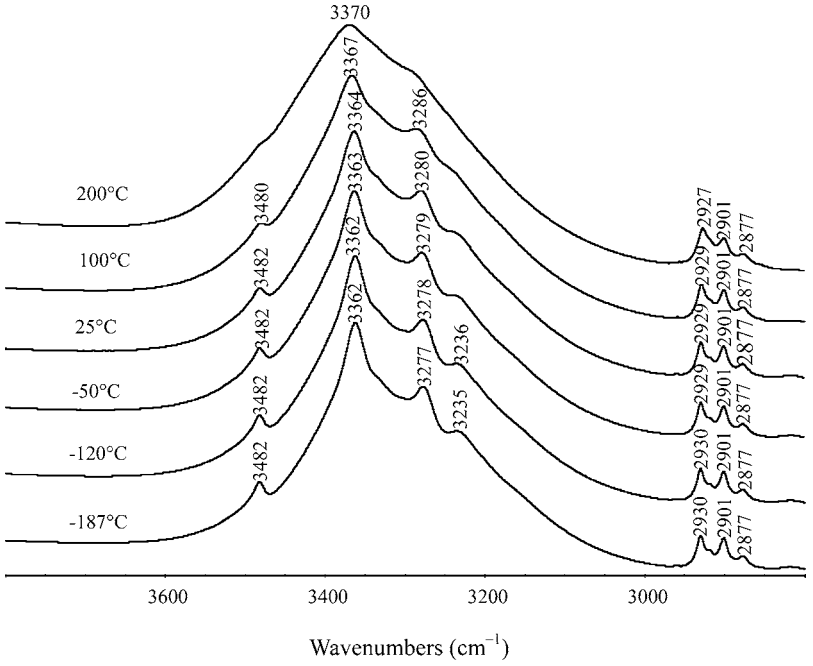

Figure 2. FTIR spectra of CsCl–*myo*-inositol complex at different temperatures (°C) in the 3800–2800 cm^{-1} region.

of the reported crystal structures of metal–sugar complexes in the neutral state are related to calcium and lanthanide ions because they have relatively stronger interactions with carbohydrates.[43–49] Na and K ions are the most important metal ions in vivo, and they often exhibit different properties. No crystal structure of potassium with carbohydrates is available at present. The crystal structures of sodium ion–carbohydrate complexes are limited,[50–53] which is not enough to serve as a reference for the structure of K with saccharides. In the periodic table of the elements, K is located between Na and Cs. K with saccharide may demonstrate properties between those of Na–saccharide and Cs–saccharide. Thus, the structures of Cs–saccharide complexes are helpful in understanding the physiological nature of K–saccharide interactions.

Here the complicated structures of cesium chloride–D-ribose (denoted as Cs-R) and cesium chloride–*myo*-inositol (denoted as Cs-I), different from those of calcium and lanthanide ions, are reported. Single crystals of metal–sugar complexes are difficult to prepare. IR, Raman, FIR, and THz spectra may provide information regarding complex formation; therefore, here the relationship between these spectra and crystal structure results is also discussed.

EXPERIMENTAL SECTION

Materials and Methods. CsCl, D-ribose, and *myo*-inositol were purchased from commercial sources and were used without further purification. The procedures of preparation of the cesium chloride–D-ribose complex (Cs-R) and cesium chloride–*myo*-inositol complex (Cs-I) were as follows: 3 mmol of D-ribose (or 3 mmol of *myo*-inositol) and 3 mmol of cesium chloride were dissolved in H_2O/ethanol and heated on a water bath at about 80 °C. Small aliquots of EtOH (Analytical Reagent) were periodically added to the solution during the heating process to prolong the reaction time, leading to the formation of the complexes. Then the concentrated solutions were cooled for crystallization. Anal. Calcd for Cs-R ($CsCl·C_5H_{10}O_5$): C, 18.86; H, 3.16. Found: C, 18.81; H, 3.16. Anal. Calcd for Cs-I ($CsCl·C_6H_{12}O_6$): C, 20.68; H, 3.47. Found: C, 20.59; H, 3.34.

Physical Measurements. Data for Cs-R were collected on a Rigaku MM007HF Saturn 724+ spectrometer using a rotating anode (λ = 0.71073 Å) at 173(2) K. Data for Cs-I were collected on a Gemini E X-ray single-crystal diffractometer using a fine-focus sealed tube (λ = 0.71073 Å) at 105(2) K. Single crystals of Cs-I were mounted in inert oil and transferred to the cold gas stream of the

Table 1. Crystal Data and Structure Refinement Details for Cesium Chloride–D-Ribose and Cesium Chloride–*myo*-Inositol Complexes

	Cs-R	Cs-I
empirical formula	$CsCl·C_5H_{10}O_5$	$CsCl·C_6H_{12}O_6$
CCDC no.	896834	916101
formula wt	318.49	348.52
T (K)	173(2)	105(2)
cryst syst, space group	orthorhombic, $P2_12_12_1$	monoclinic, $P2_1/n$
unit cell dimens		
a (Å)	6.7596(14)	6.8047(11)
b (Å)	8.8699(18)	18.747(2)
c (Å)	15.191(3)	8.4936(15)
α (deg)	90	90
β (deg)	90	106.44(2)
γ (deg)	90	90
V (Å^3)	910.8(3)	1039.3(3)
no. of collected/unique rflns	9319/2069	4258/2047
R_{int}	0.0589	0.0424
Z; calcd density (Mg/m^3)	4; 2.323	4; 2.227
abs coeff (mm^{-1})	4.341	3.822
F(000)	608	672
cryst size (mm^3)	0.35 × 0.34 × 0.18	0.50 × 0.40 × 0.01
θ range for data collection (deg)	2.66–27.47	3.31–26.00
limiting indices	$-8 \le h \le 8, -11 \le k \le 11, -19 \le l \le 19$	$-8 \le h \le 8, -23 \le k \le 12, -10 \le l \le 10$
completeness to θ_{max}, %	99.2	99.8
no. of data/restraints/params	2069/0/109	2047/17/147
goodness of fit on F^2	1.129	1.106
final R indices ($I > 2\sigma(I)$)	R1 = 0.0251, wR2 = 0.0645	R1 = 0.0486, wR2 = 0.1202
R indices (all data)	R1 = 0.0253, wR2 = 0.0646	R1 = 0.0567, wR2 = 0.1250
largest diff peak, hole, e Å^{-3}	0.630, −1.246	1.964, −1.340

dx.doi.org/10.1021/ic402027j | Inorg. Chem. 2013, 52, 13132–13145

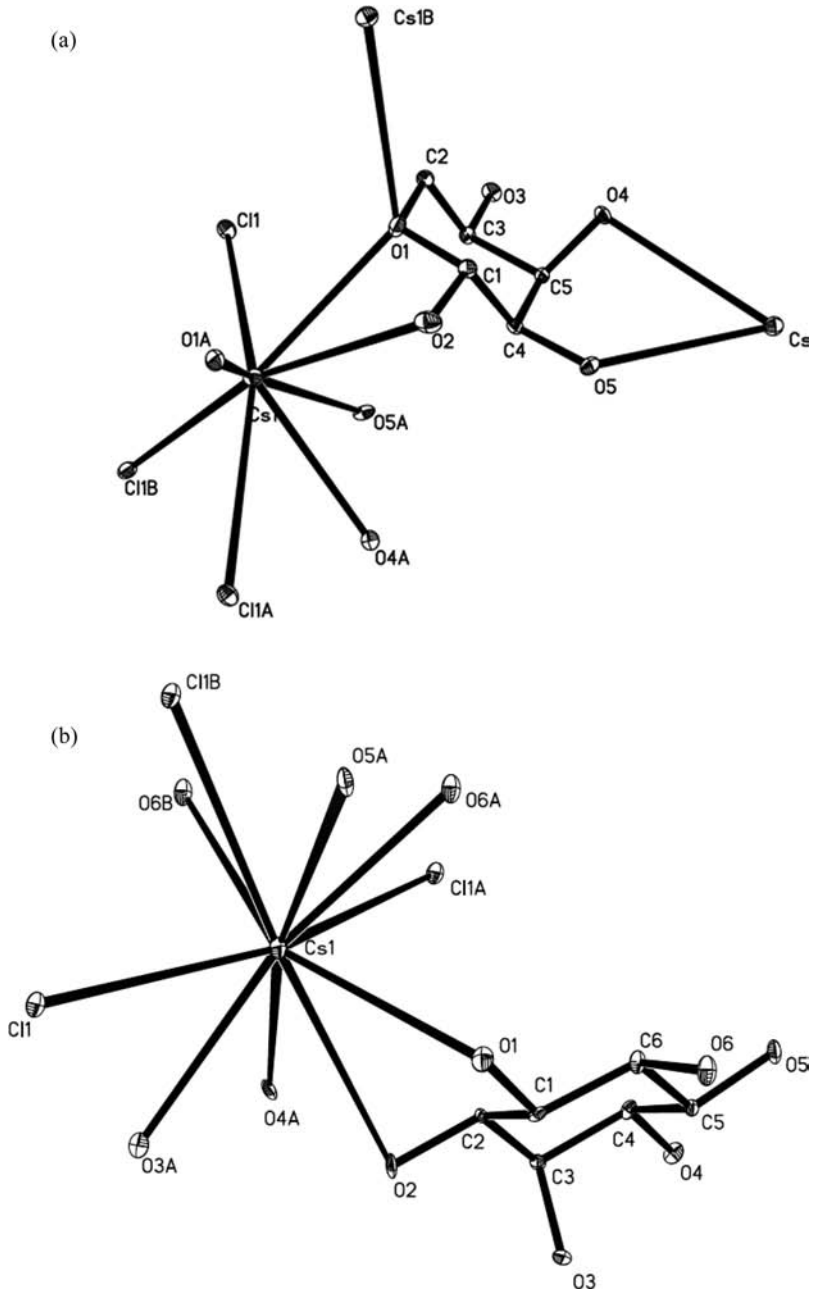

Figure 3. Crystal structures of CsCl–D-ribose (a) and CsCl–*myo*-inositol complexes (b).

diffractometer. The structures were resolved by direct methods with SHELX-97 and refined using the full-matrix least squares on F^2 method. Anisotropic thermal parameters were used for the non-hydrogen atoms and isotropic parameters for the hydrogen atoms. Hydrogen atoms were added geometrically and refined using a riding model.[54]

The mid-IR spectra in the 4000–600 cm^{-1} region were measured on a Nicolet Magna IN10 spectrometer using the micro-IR method at 4 cm^{-1} resolution and 64 scans. The variable-temperature FTIR spectra of Cs-I were measured on a Bruker VERTEX 80v FTIR spectrometer with a variable-temperature attachment at 4 cm^{-1} resolution and 32 scans. The elemental analyses were carried out on an Elementar Vario EL spectrometer. The THz absorption spectra in the 0.2–2.5 THz region were recorded on the THz time-domain device of the Capital Normal University of China. The experimental apparatus for terahertz transmission measurements was discussed in detail elsewhere.[55] The far-IR spectra of the molecules in the 650–50 cm^{-1} region were measured by the commonly used Nujol mull method and were taken on a Nicolet Magna-IR 750 II spectrometer at room temperature and at 8 cm^{-1} resolution and 128 scans. The Raman spectra were recorded on a Nicolet 6700 FTIR NXR FT-Raman module at 4 cm^{-1} resolution and 256 scans.

RESULTS AND DISCUSSION

FTIR Spectra of Cesium Chloride–D-Ribose and Cesium Chloride–*myo*-Inositol Complexes. The FTIR spectra of D-ribose, cesium chloride–D-ribose complex, *myo*-inositol, and cesium chloride–*myo*-inositol complex are shown in Figure 1. In comparison to the IR spectrum of D-ribose,[56–58] the changes in the IR spectrum of Cs-R indicate the formation of cesium chloride–D-ribose complex. For the spectrum of Cs-R, in the 3600–2600 cm^{-1} region, 3426, 3333, 3251, and 3182 cm^{-1} bands are observed (3418, 3358, and 3210 cm^{-1} bands for D-ribose), which are related to the hydrogen bonds after

dx.doi.org/10.1021/ic402027j | *Inorg. Chem.* 2013, 52, 13132–13145

Table 2. Selected Bond Lengths (Å) and Angles (deg) for Cesium Chloride−D-Ribose Complex[a]

Cs1−O5	3.200(3)	C2−O1	1.424(5)
Cs1−O4	3.242(3)	C2−C3	1.528(6)
Cs1−O1	3.248(3)	O1−C1	1.446(5)
Cs1−O2	3.316(4)	O2−C1	1.380(5)
Cs1−Cl1	3.4055(12)	O3−C3	1.435(4)
Cs1−Cl1#2	3.4197(12)	O4−C5	1.431(5)
Cs1−O1#3	3.423(3)	O5−C4	1.428(5)
Cs1−Cl1#4	3.5055(12)	C1−C4#7	1.532(5)
Cl1−Cs1#5	3.4197(12)	C3−C5#7	1.524(5)
Cl1−Cs1#6	3.5055(12)	C4−C5	1.525(5)
O1−Cs1#1	3.423(3)	C4−C1#8	1.532(5)
C5−C3#8	1.524(5)		
O1−C2−C3	109.7(3)	O4−Cs1−Cl1	122.07(5)
O1−C2−Cs1#1	72.9(2)	O1−Cs1−Cl1	68.56(5)
C3−C2−Cs1#1	166.5(3)	O2−Cs1−Cl1	108.76(6)
O5−Cs1−O4	50.90(7)	O5−Cs1−Cl1#2	75.73(6)
O5−Cs1−O1	79.49(8)	O4−Cs1−Cl1#2	82.38(5)
O4−Cs1−O1	101.89(7)	O1−Cs1−Cl1#2	143.79(6)
O5−Cs1−O2	93.60(8)	O2−Cs1−Cl1#2	164.63(6)
O4−Cs1−O2	82.30(8)	Cl1−Cs1−Cl1#2	78.67(2)
O1−Cs1−O2	40.23(8)	O5−Cs1−O1#3	152.00(7)
O5−Cs1−Cl1	71.40(6)	O4−Cs1−O1#3	109.31(7)
O2−Cs1−O1#3	61.39(7)	O1−Cs1−O1#3	87.32(5)
Cl1−Cs1−O1#3	126.20(5)	O1#3−Cs1−Cl1#4	70.46(5)
Cl1#2−Cs1−O1#3	125.65(5)	O5−Cs1−C2#3	158.66(9)
O5−Cs1−Cl1#4	101.48(6)	O4−Cs1−C2#3	132.36(8)
O4−Cs1−Cl1#4	53.34(5)	O1−Cs1−C2#3	79.32(9)
O1−Cs1−Cl1#4	133.96(5)	O2−Cs1−C2#3	68.24(9)
O2−Cs1−Cl1#4	94.38(6)	Cl1−Cs1−C2#3	102.96(7)
Cl1−Cs1−Cl1#4	155.97(3)	O2−Cs1−Cs1#2	132.04(6)
Cl1#2−Cs1−Cl1#4	77.31(2)	Cl1−Cs1−Cs1#2	117.05(2)
Cl1#2−Cs1−C2#3	124.19(7)	Cl1#2−Cs1−Cs1#2	38.385(18)
O1#3−Cs1−C2#3	23.44(7)	O1#3−Cs1−Cs1#2	99.35(5)
Cl1#4−Cs1−C2#3	91.38(6)	Cl1#4−Cs1−Cs1#2	38.928(16)
O5−Cs1−Cs1#2	88.16(6)	C2#3−Cs1−Cs1#2	112.17(7)
O4−Cs1−Cs1#2	62.25(5)	O5−Cs1−Cs1#5	68.53(6)
O1−Cs1−Cs1#2	164.05(5)	O4−Cs1−Cs1#5	105.34(5)
O1−Cs1−Cs1#5	105.85(5)	Cl1#4−Cs1−Cs1#5	117.41(2)
O2−Cs1−Cs1#5	145.53(5)	C2#3−Cs1−Cs1#5	120.30(7)
Cl1−Cs1−Cs1#5	38.575(16)	Cs1#2−Cs1−Cs1#5	78.480(17)
Cl1#2−Cs1−Cs1#5	40.098(18)	C2−O1−Cs1#1	83.6(2)
O1#3−Cs1−Cs1#5	139.33(5)	C1−O1−Cs1#1	106.6(2)
Cs1−Cl1−Cs1#5	103.04(2)	Cs1−O1−Cs1#1	124.02(8)
Cs1−Cl1−Cs1#6	155.97(3)	C1−O2−Cs1	99.1(2)
Cs1#5−Cl1−Cs1#6	100.97(2)	C5−O4−Cs1	102.7(2)
C2−O1−C1	113.8(3)	C4−O5−Cs1	121.3(2)
C2−O1−Cs1	127.5(3)	O2−C1−O1	106.1(3)
C1−O1−Cs1	100.5(2)	O2−C1−C4#7	109.0(3)
O3−C3−C2	111.0(3)	O1−C1−C4#7	109.8(3)
C5#7−C3−C2	109.4(3)	O3−C3−C5#7	109.3(3)
O5−C4−C5	109.2(3)	O4−C5−C3#8	111.3(3)
O5−C4−C1#8	110.1(3)	O4−C5−C4	108.7(3)
C5−C4−C1#8	110.7(3)	C3#8−C5−C4	108.2(3)

[a]Symmetry transformations used to generate equivalent atoms: (#1) $x - {}^1/_2, -y + {}^1/_2, -z$; (#2) $x + {}^1/_2, -y + {}^3/_2, -z$; (#3) $x + {}^1/_2, -y + {}^1/_2, -z$; (#4) $x + 1, y, z$; (#5) $x - {}^1/_2, -y + {}^3/_2, -z$; (#6) $x - 1, y, z$; (#7) $-x + 2, y - {}^1/_2, -z + {}^1/_2$; (#8) $-x + 2, y + {}^1/_2, -z + {}^1/_2$.

complexation. Weak bands at 2983, 2941, 2915, 2873, 2860, and 2821 cm^{-1} for Cs-R (2943, 2919, and 2876 cm^{-1} bands for D-ribose) are related to ν(CH). The changes in peak positions and the decrease of relative intensities of ν(CH) indicate the formation of metal complexes and rearrangement of the CH chain. No bands can be observed in the 1700−1600 cm^{-1} region, which indicates that no water exists in the structure of Cs-R.

The peak positions and relative intensities of the bands in the 1500−600 cm^{-1} region for Cs-R are changed in comparison to D-ribose, which indicates the formation of a metal complex.

dx.doi.org/10.1021/ic402027j | Inorg. Chem. 2013, 52, 13132−13145

Table 3. Selected Bond Lengths (Å) and Angles (deg) for Cesium Chloride−*myo*-Inositol Complex[a]

Cs1−O1	3.249(5)	O3−Cs1#8	3.361(4)
Cs1−Cl1	3.4276(16)	O3−C3	1.430(7)
Cs1−Cl1#2	3.4996(16)	O6−Cs1#9	3.151(4)
Cs1−Cl1#3	3.6690(15)	O6−Cs1#5	3.138(4)
Cs1−O2	3.495(4)	O6−C6	1.439(7)
Cs1−O3#4	3.361(4)	C1−C6	1.520(8)
Cs1−O6#5	3.138(4)	C1−C2	1.513(8)
Cs1−O6#6	3.151(4)	C6−C5	1.535(8)
Cs1−O5#5	3.621(4)	C2−C3	1.518(7)
Cs1−O4#4	3.415(4)	C3−C4	1.538(7)
O1−C1	1.435(7)	O5−Cs1#5	3.621(4)
Cl1−Cs1#3	3.6690(15)	O5−C5	1.429(6)
Cl1−Cs1#7	3.4996(16)	O4−Cs1#8	3.415(4)
O2−C2	1.439(6)	O4−C4	1.450(7)
		C5−C4	1.492(8)
O1−Cs1−Cs1#1	111.14(8)	O6#6−Cs1−C2	127.36(11)
O1−Cs1−Cl1	117.17(9)	O6#5−Cs1−C2	85.21(11)
O1−Cs1−Cl1#2	83.44(9)	O6#5−Cs1−O5#5	48.60(10)
O1−Cs1−Cl1#3	124.10(7)	O6#6−Cs1−O5#5	99.77(10)
O1−Cs1−O2	49.61(10)	O6#6−Cs1−O4#4	87.72(11)
O1−Cs1−O3#4	100.32(10)	O6#5−Cs1−O4#4	124.59(10)
O1−Cs1−C2	39.55(11)	C2−Cs1−Cs1#1	111.05(8)
O1−Cs1−O5#5	75.04(10)	O5#5−Cs1−Cs1#1	70.41(7)
O1−Cs1−O4#4	94.45(10)	O5#5−Cs1−Cl1#3	49.68(7)
Cl1−Cs1−Cs1#1	119.37(3)	O5#5−Cs1−C2	112.15(10)
Cl1#3−Cs1−Cs1#1	48.53(3)	O4#4−Cs1−Cs1#1	111.13(7)
Cl1#2−Cs1−Cs1#1	51.77(3)	O4#4−Cs1−Cl1#2	70.84(7)
Cl1#2−Cs1−Cl1#3	100.30(3)	O4#4−Cs1−Cl1	99.59(7)
Cl1−Cs1−Cl1#2	158.42(5)	O4#4−Cs1−Cl1#3	139.85(7)
Cl1−Cs1−Cl1#3	74.18(4)	O4#4−Cs1−O2	46.14(10)
Cl1−Cs1−O2	108.16(7)	O4#4−Cs1−C2	56.78(11)
Cl1#2−Cs1−C2	62.19(9)	O4#4−Cs1−O5#5	168.88(9)
Cl1#3−Cs1−C2	153.47(9)	C1−O1−Cs1	117.4(3)
Cl1−Cs1−C2	129.46(9)	Cs1#7−Cl1−Cs1#3	79.70(3)
Cl1−Cs1−O5#5	88.65(7)	Cs1−Cl1−Cs1#3	105.82(4)
Cl1#2−Cs1−O5#5	103.78(7)	Cs1−Cl1−Cs1#7	158.42(5)
O2−Cs1−Cs1#1	131.04(6)	C2−O2−Cs1	90.4(3)
O2−Cs1−Cl1#3	173.71(7)	C3−O3−Cs1#8	106.4(3)
O2−Cs1−Cl1#2	79.63(7)	Cs1#5−O6−Cs1#9	93.87(11)
O2−Cs1−C2	22.32(10)	C6−O6−Cs1#5	117.6(3)
O2−Cs1−O5#5	124.13(9)	C6−O6−Cs1#9	136.3(3)
O3#4−Cs1−Cs1#1	144.42(7)	O1−C1−C6	107.8(5)
O3#4−Cs1−Cl1#3	123.65(7)	O1−C1−C2	111.4(4)
O3#4−Cs1−Cl1	54.07(7)	C2−C1−C6	110.4(4)
O3#4−Cs1−Cl1#2	119.14(7)	O6−C6−C1	110.3(5)
O3#4−Cs1−O2	60.94(9)	O6−C6−C5	106.1(4)
O3#4−Cs1−C2	82.87(10)	C1−C6−C5	112.4(5)
O3#4−Cs1−O5#5	136.20(9)	O2−C2−Cs1	67.3(3)
O3#4−Cs1−O4#4	48.31(9)	O2−C2−C1	107.8(4)
O6#5−Cs1−Cs1#1	43.17(8)	O2−C2−C3	111.1(5)
O6#6−Cs1−Cs1#1	42.95(8)	C1−C2−Cs1	91.3(3)
O6#6−Cs1−O1	151.47(12)	C1−C2−C3	110.9(4)
O6#5−Cs1−O1	69.26(11)	C3−C2−Cs1	156.3(4)
O6#5−Cs1−Cl1#3	68.26(8)	O3−C3−C2	111.4(4)
O6#5−Cs1−Cl1#2	55.30(8)	O3−C3−C4	107.1(4)
O6#6−Cs1−Cl1#2	70.40(8)	C2−C3−C4	109.5(5)
O6#6−Cs1−Cl1#3	53.36(8)	C5−O5−Cs1#5	114.0(3)
O6#5−Cs1−Cl1	135.41(8)	C4−O4−Cs1#8	121.6(3)
O6#6−Cs1−Cl1	90.34(8)	O5−C5−C6	109.1(5)
O6#6−Cs1−O2	131.68(10)	O5−C5−C4	109.3(5)
O6#5−Cs1−O2	107.07(10)	C4−C5−C6	110.6(4)
O6#6−Cs1−O3#4	102.23(11)	O4−C4−C3	108.0(5)

dx.doi.org/10.1021/ic402027j | *Inorg. Chem.* 2013, 52, 13132−13145

Table 3. continued

O6#5−Cs1−O3#4	168.00(10)	O4−C4−C5	111.3(4)
O6#5−Cs1−O6#6	86.13(11)	C5−C4−C3	111.1(4)

[a]Symmetry transformations used to generate equivalent atoms: (#1) $1-x, -y, 1-z$; (#2) $-1+x, +y, +z$; (#3) $2-x, -y, 1-z$; (#4) $^1/_2+x, {}^1/-y, -^1/_2+z$; (#5) $1-x, -y, 2-z$; (#6) $+x, +y, -1+z$; (#7) $1+x, +y, +z$; (#8) $-^1/_2+x, {}^1/-y, {}^1/_2+z$; (#9) $+x, +y, 1+z$.

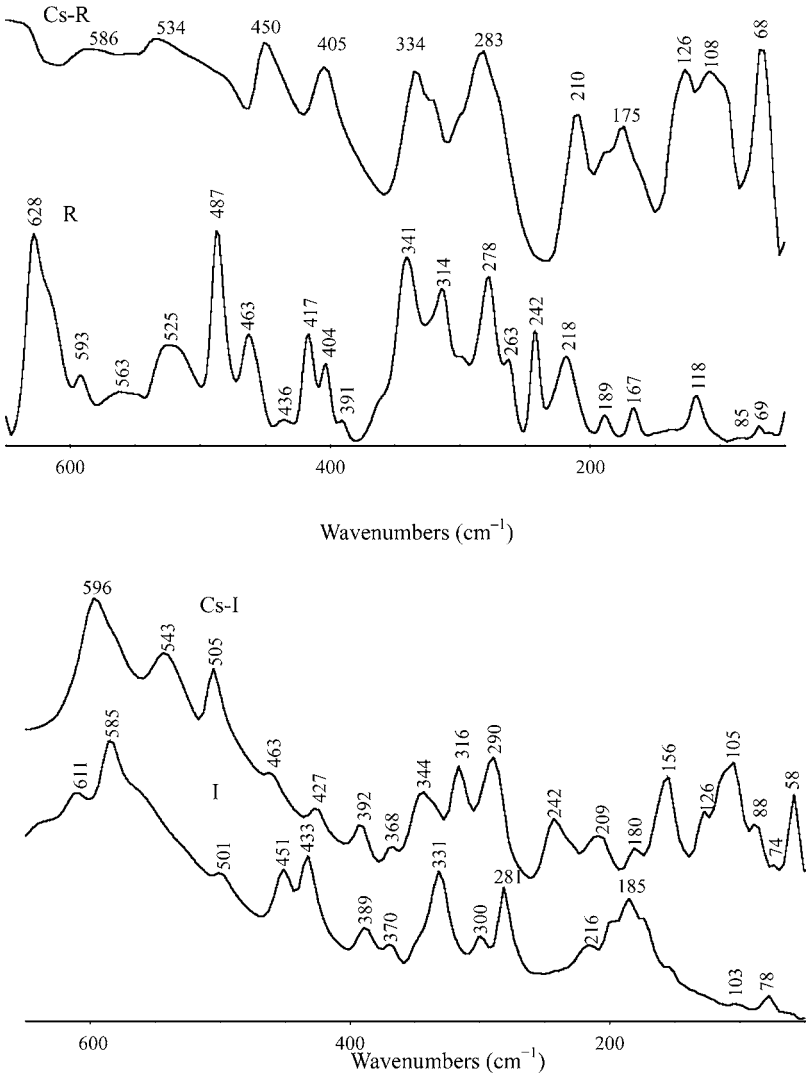

Figure 4. FIR spectra of D-ribose, CsCl−D-ribose complex, *myo*-inositol, and CsCl−*myo*-inositol complex in the 650−50 cm^{-1} region.

$\delta(CH_2)$ has shifted from 1452 cm^{-1} in D-ribose to 1455 cm^{-1} in Cs-R. The out-of-plane deformation (wagging) of CH_2, 1380 and 1363 cm^{-1} for D-ribose, is shifted to lower frequencies, 1361 and 1330 cm^{-1} ,in the spectrum of the complex. The $\nu(CO)$ vibrations localized at 1161−1117 cm^{-1} in the D-ribose spectrum are shifted toward lower frequencies at 1153, 1136, 1118, and 1102 cm^{-1} in the Cs−D-ribose spectrum. The $\delta(COH)$ band at 1032 cm^{-1} is observed at 1052 and 1030 cm^{-1} upon salt formation, which indicates the coordination of hydroxyl groups to Cs^+ ion. The skeleton deformation bands, mainly at about 1000−400 cm^{-1} in the spectrum of D-ribose, show considerable changes upon metalation. The bands at 958, 922, and 911 cm^{-1} in the free D-ribose spectrum are shifted to 950 and 917 cm^{-1}. Those bands at 869, 804, and 727 cm^{-1} appear at 867 and 734 cm^{-1} upon Cs^+ salt formation. In comparison to the IR spectrum of Cs-R with lanthanide−D-ribose complexes, Pr-R ($PrCl_3$−D-ribose), Nd-R, and Sm-R, etc., the changes in the IR spectra are different because the coordination mode of D-ribose is varied. For example, in the IR spectrum of PrR, the $\nu(OH)$ vibrations are broad bands and $\nu(CH)$ bands are weak, but four obvious $\nu(OH)$ bands can be observed in Cs-R and the relative intensities of ν_{CH} in Cs-R are stronger than those for Pr-R, which indicates that the hydrogen bonds and CH chains are different in Pr-R and Cs-R. In the 1500−650 cm^{-1} region the number of the bands are similar for Cs-R and Pr-R, but the peak positions and relative intensities of the bands are different in Cs-R and Pr-R. Three bands at 1153, 1030, and 950 cm^{-1} are stronger bands in Cs-R, and 1048 and 1004 cm^{-1} bands are stronger in Pr-R. Other differences of PrR and Cs-R are related to the existence of water molecules. The bands at 1632 and 1619 cm^{-1} related to $\delta(H_2O)$ in Pr-R are absent in Cs-R. The IR spectra indicate the formation of cesium chloride−D-ribose complex and changes in the hydrogen bonds and also show that cesium, calcium, and lanthanide ions have different coordination structures.

dx.doi.org/10.1021/ic402027j | *Inorg. Chem.* 2013, 52, 13132−13145

The FTIR spectra of *myo*-inositol and cesium chloride−*myo*-inositol complex shown in Figure 1 indicate the formation of cesium chloride−*myo*-inositol complex. In the IR spectrum of *myo*-inositol, the ν(OH) vibrations are located at 3388, 3377, 3316, and 3236 cm^{-1}, and the bands are shifted to 3487, 3331, and 3284 cm^{-1} in cesium chloride−*myo*-inositol complex, which indicate changes in the hydrogen bonds after complexation. The small band at 3487 cm^{-1} should be related to longer hydrogen bonds. The ν(CH) vibrations are located at 2960, 2923, and 2903 cm^{-1} in *myo*-inositol, and the bands are shifted to 2930, 2905, 2879, and 2820 cm^{-1} in cesium chloride−*myo*-inositol complex, which indicate changes in the CH chain of *myo*-inositol. There is no band at ∼1640 cm^{-1}, which shows that no water exists in the structure of cesium chloride−*myo*-inositol complex. The $\delta(CH_2)$ bands at 1445 and 1417 cm^{-1} are shifted to 1475 and 1413 cm^{-1}, which also indicate changes in the CH chain. The bands in the fingerprint region also show fine structures after complexation, which indicate the formation of the metal complex. For example, the bands at 1371, 1357, and 1324 cm^{-1} related to ν(CC), δ(CCH), δ(CCO), δ(COH), and ι(CCCH)[59] are shifted to 1389, 1369, 1355, and 1318 cm^{-1}, which indicate the conformation changes of the ligand. The bands at 1246 and 1220 cm^{-1} mainly related to δ(COH) and ν(CO) in *myo*-inositol correspond to 1246 and 1229 cm^{-1} in Cs-I. The bands at 1196, 1147, 1114, 1049, 1014, and 1002 cm^{-1} are mainly related to ν(CO) and ν(CC) vibrations. After complexation the bands are shifted to 1190, 1151, 1136, 1121, 2092, 1071, 1035, and 1011 cm^{-1}, which indicates the coordination of hydroxyl groups of the ligand. Other bands also shifted to higher or lower wavenumbers and show the formation of the metal complex. In comparison with the IR spectra of lanthanide−*myo*-inositol complexes, the different changes in peak positions and relative intensities indicate the various coordination modes of *myo*-inositol.

For investigation of the hydrogen bonds, the variable-temperature FTIR spectra of Cs-I have been measured and are shown in Figure 2. In the 3600−3000 cm^{-1} region, the bands at 3482 and 3235 cm^{-1} related to hydrogen bonds are relatively more evident, but no new band appears at low temperature. At high temperature three bands become one, which are related to the change of the hydrogen bonds along with temperature.

Crystal Structures of Cesium Chloride−D-Ribose and Cesium Chloride−*myo*-Inositol Complexes. The crystal structures of cesium chloride−D-ribose and cesium chloride−*myo*-inositol complexes are shown in Figure 3. For clarity, not all H atoms are shown here. The crystal data and structure refinements of Cs-R and Cs-I complexes are given in Table 1. The selected bond lengths and bond angles for Cs-R and Cs-I complexes are given in Table 2 and 3, respectively.

Cs^+ is eight-coordinated to three chloride ions and five hydroxyl groups from three D-ribose molecules, including O1 and O2 from one D-ribose molecule, O1 from another D-ribose molecule, and O4 and O5 from the third D-ribose molecule in Cs-R. For one D-ribose molecule, the oxygen atom O1 in the ring is coordinated to two cesium ions as an oxygen bridge, O2 is coordinated to one of the cesium ions, and O4 and O5 are coordinated to the third cesium ion, respectively. O3 does not coordinate to metal ions and only takes part in forming hydrogen bonds. One chloride ion is connected to three cesium ions here. Thus, a complicated structure of Cs−D-ribose forms. Cs−O distances are from 3.200 to 3.423 Å; the average Cs−O distance is 3.286 Å. Cs−Cl distances are 3.4055, 3.4197, and 3.5055 Å. D-Ribose has a coordination mode in Cs-R relatively

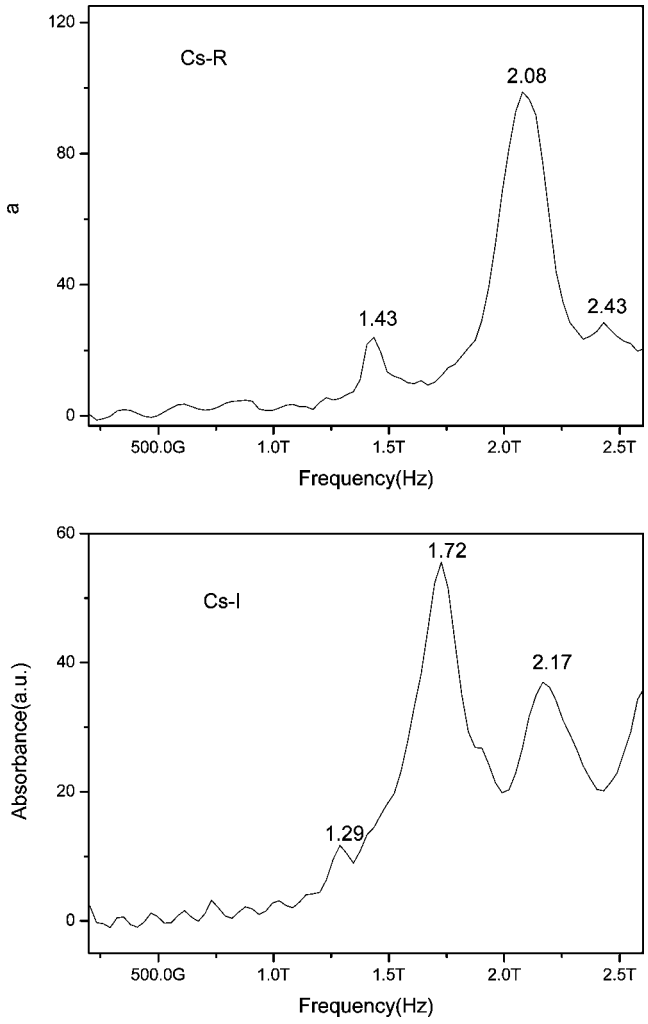

Figure 5. THz spectra of CsCl−D-ribose and CsCl−*myo*-inositol complexes.

more complicated than in the corresponding lanthanide−D-ribose complex ($LnCl_3{\cdot}C_5H_{10}O_5{\cdot}5H_2O$), in which D-ribose provides three hydroxyl groups to coordinate to metal ions and the oxygen atom in the ring does not coordinate to metal ions.[24−28,31,32] The structure of Cs-R is also different from that of calcium−D-ribose complex ($CaCl_2{\cdot}C_5H_{10}O_5{\cdot}3H_2O$), in which calcium ion is coordinated to O1, O2, and O3 of one D-ribose molecule and O4 and O5 from the second D-ribose molecule.[29]

The C−C bond lengths are 1.532, 1.528, 1.524, 1.525, and 1.532 Å, C−O bond lengths are 1.424, 1.446, 1.380, 1.435, 1.431, and 1.428 Å, O−C−C bond angles are 108.7, 109.0, 109.2, 109.8, 109.7, 109.3, 110.1, 111.0, and 111.3°, C−C−C bond angles are 108.2, 109.4, and 110.7°, and the bond angle of C2−O1−C1 is 113.8° for cesium chloride−D-ribose complex. Here D-ribose keeps a chair conformation in its six-membered rings, but it is different from that in lanthanide complexes, in which D-ribose has $^1C_4$ and $^4C_1$ conformations. The ribose moiety exists as a furanose with α-D configuration in calcium chloride−D-ribose complex. Here in Cs-R, in the six-membered ring conformation of D-ribose, if we let the ring oxygen O1 locate at the plane of the chair, then three C atoms in the plane of the chair are connected to three hydroxyl groups, which makes the conformation is different from that α-D-pyranose ($^1C_4$ and $^4C_1$) and β-D-pyranose ($^1C_4$ and $^4C_1$), in which the plane of the chair is formed by oxygen and three C atoms with

dx.doi.org/10.1021/ic402027j | Inorg. Chem. 2013, 52, 13132−13145

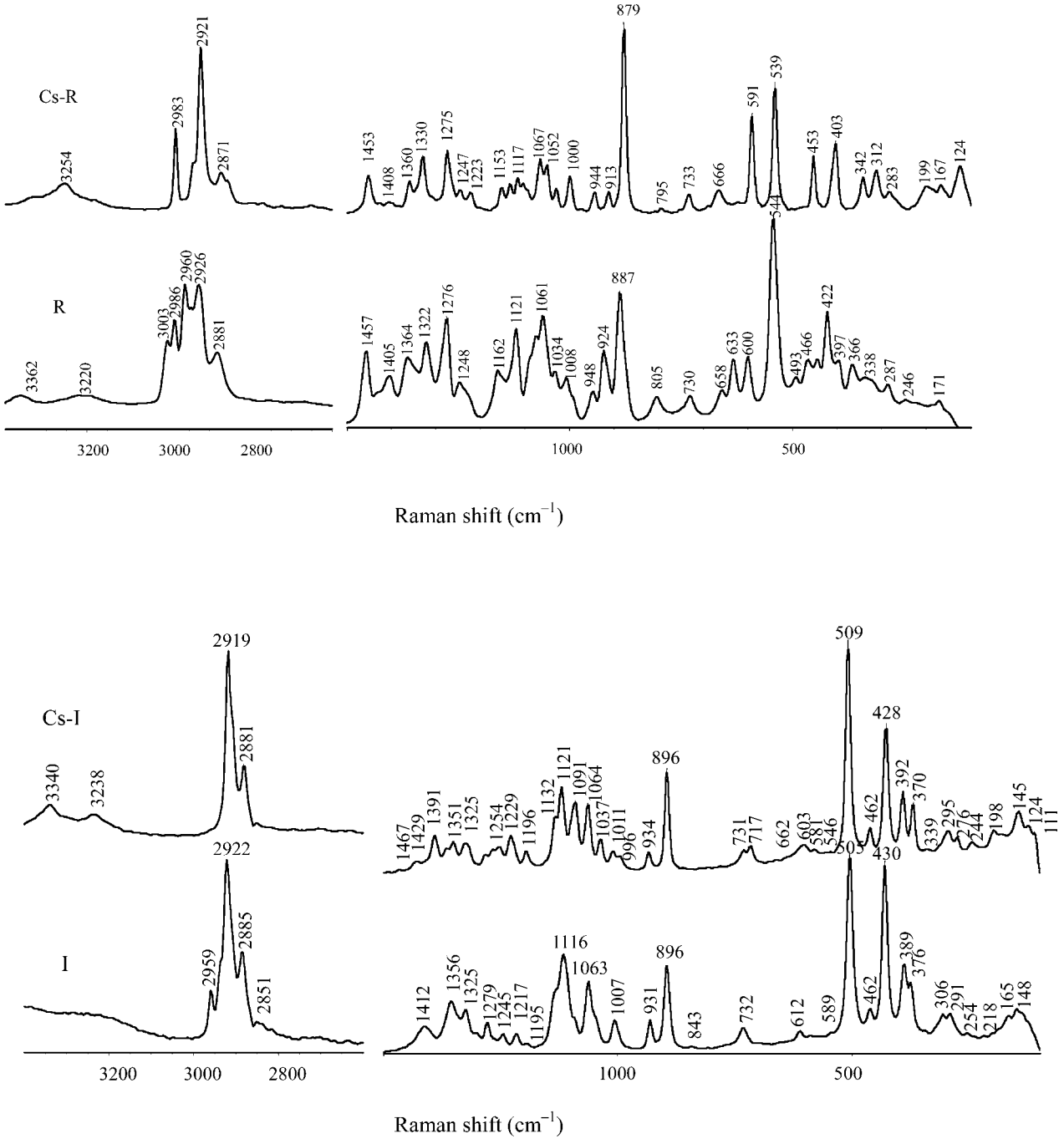

Figure 6. Raman spectra of D-ribose, CsCl−D-ribose complex, *myo*-inositol, and CsCl−*myo*-inositol complex in the 3400−2600 and 1500−100 cm^{-1} regions.

two hydroxyl groups. The change in conformation of D-ribose is to favor coordination with cesium ion. The differences may be due to the influence of ionic radius and charge. The ionic radius of the cesium ion is 1.67 Å, which is larger than that of Ca^{2+} (0.99 Å), and it is a monovalent metal ion; therefore, D-ribose adopts a new coordination mode, which shows the influence of different metal ions. The torsion angle Cl1#4−Cs1−Cl1−Cs1#6 is 180.0°, and that of Cl1#2−Cs1−Cl1−Cs1#5 is 0.0°, which indicates that Cs and Cl atoms are in a plane.

The hydrogen bond data show that there are O−H···O and O−H···Cl hydrogen bonds in Cs-R. The uncoordinated hydroxyl group O3 forms hydrogen bonds with coordinated hydroxyl groups O4 and O5. Considering the ν(OH) bands in the 3500−3000 cm^{-1} region in its IR spectrum, the preliminary assignments may be as follows: the 3426 cm^{-1} band may be related to O2−H···Cl1 ($x + {}^1/_2, -y + {}^1/_2, -z$) (the O−H···Cl angle is 171.1°, and the distance between oxygen and chloride atoms is 3.077 Å), the 3333 cm^{-1} band may be related to O4−H···Cl1 ($x + 1, y, z$) (170.0°, 3.038 Å), the 3251 cm^{-1} band may be related to O5−H···O3 [$-x + 1, y + {}^1/_2, -z + {}^1/_2$] (169.8°, 2.851 Å), and the 3182 cm^{-1} band may be related to O3−H···O4 ($x - 1, y, z$) (158.5°, 2.773 Å).

D-Ribose is a relatively simple ligand, but several coordination modes are observed. For Ca^{2+}, D-ribose has a furanose form with α-D configuration, for lanthanide ions, *ax-eq-ax* pyranose conformations are presented, and for cesium ion, a

dx.doi.org/10.1021/ic402027j | *Inorg. Chem.* 2013, 52, 13132−13145

new conformation is obtained; in particular, the oxygen atom in the ring of D-ribose is coordinated to two cesium ions. Lanthanide ions have smaller ionic radii and three charges, and they usually have high coordination numbers; therefore, they can accept three hydroxyl groups from one D-ribose in their coordination spheres.[24−28,31,32] The differences in coordination modes of D-ribose are related to the charge and ionic radius of metal ions.

The structure of cesium chloride−*myo*-inositol complex is more complicated than that of Cs-R. For the ligand, one *myo*-inositol is connected to four metal ions; its O1 and O2 atoms are coordinated to one cesium ion, O3 and O4 are coordinated to the second cesium ion, O5 and O6 are coordinated to the third cesium ion, and O6 is also coordinated to the fourth cesium ion, respectively. Correspondingly, one metal ion is connected to four ligands: i.e., Cs^+ is 10-coordinated to three bridging chloride ions and seven hydroxyl groups from four *myo*-inositol molecules, including O1 and O2 from one *myo*-inositol molecule, O3 and O4 from the second *myo*-inositol molecule, O5 and O6 from the third *myo*-inositol molecule, and O6 from the fourth *myo*-inositol in Cs-I. Thus, a complicated network forms. The structure of cesium chloride−*myo*-inositol complex is different from those of calcium−, magnesium−, and lanthanide−*myo*-inositol complexes, in which *myo*-inositol is a bidentate ligand (O1 and O2 *cis* vicinal hydroxyl groups in MgI and LnI, O2 and O3 hydroxyl groups (an axial−equatorial pair) or O5 and O6 hydroxyl groups (an equatorial-equatorial pair) in $CaBr_2{\cdot}2C_6H_{12}O_6{\cdot}5H_2O$). *myo*-Inositol has a relatively complicated coordination mode in the cesium complex.

The Cs−O distances are from 3.138 to 3.621 Å, and Cs−Cl distances are 3.428, 3.500, and 3.669 Å, respectively. The C−C bond lengths are 1.492, 1.520, 1.513, 1.535, 1.518, and 1.538 Å, C−O bond lengths are 1.435, 1.430, 1.429, 1.439, and 1.450 Å, O−C−C bond angles are 106.1, 107.1, 107.8, 108.0, 109.1, 109.3, 110.3, 111.1, 111.,3 and 111.4°,and C−C−C bond angles are 109.5, 110.4, 110.6, 110.9, 111.,1 and 112.4° in Cs-I, respectively. The C−O and C−C distances and the bond angles of *myo*-inositol and its metal complexes are given in Table S1 (Supporting Information). When the data of Cs-I are compared with those of CaI, MgI, and Ln-I, the average C−O distance of Cs-I is 1.4395 Å and is the longest distance (1.43 Å in CaI, 1.4307 Å in MgI, 1.4293 in PrI, 1.4247 in NdI), which may be related to the large radius of the cesium ion. The shortest and longest C−C distances, 1.492 and 1.538 Å, appear in Cs-I, which is related to the complicated coordination mode of *myo*-inositol. The C−C−C bond angles are 109.5−112.4° in Cs-I, which is a relatively small change (110.1−112.9° in CaI, 109.9−114.2° in MgI, 110.0−113.5° in Pr,I and 111.0−114.1° in NdI). Some of the O−C−C bond angles, for example, O1−C1−C2, O2−C2−C3, O3−C3−C4, and O5−C5−C6, have larger changes due to its special coordination mode. The metal−hydroxyl interactions produce small conformational changes in the sugar at the metal binding sites. The chair conformation of *myo*-inositol has been retained in the structure of Cs-I.

The hydrogen bond data show that all of the hydroxyl groups of *myo*-inositol are involved in forming hydrogen bonds, including O−H···O and O−H···Cl hydrogen bonds. The bands at 3487, 3331, and 3284 cm^{-1} assigned to ν(OH) are related to the hydrogen bonds, including O1−H1···O6 (110.48°, 2.867 Å), O2−H1B···O4 ($x + {}^1/_2, -y + {}^1/_2, z - {}^1/_2$) (170.22°, 2.709 Å), O3−H3···Cl1 ($x - {}^1/_2, -y + {}^1/_2, z + {}^1/_2$) (153.92°, 3.086 Å), O5−H5···Cl1 ($x - 1, y, z + 1$) (175.55°, 3.063 Å), O4−H4···O2 ($x - 1, y, z$) (164.74°, 2.712 Å), and O6−H6···Cl1 ($-x + 2, -y, -z + 2$) (134.31°, 3.097 Å). The torsion angles Cl1#7− Cs1−Cl1−Cs1#2

Table 4. Coordination Modes of the Metal−D-Ribose (M-R) and −*myo*-Inositol (M-I) Complexes

stoichiometry	example	CN	space group	OH	coordination mode of the ligand	H_2O	Cl^-
$CaBr_2{\cdot}2C_6H_{12}O_6{\cdot}5H_2O$	Ca-I	8	$P\bar{1}$	4	O2 and O3 hydroxyl groups (an axial−equatorial pair) to M1; O5 and O6 hydroxyl groups (an equatorial−equatorial pair) to M1	4 coordinated, 1 hydrogen-bonded	
$MgCl_2{\cdot}C_6H_{12}O_6{\cdot}4H_2O$	Mg-I	6	$P2_1/c$	2	O1 and O2 *cis* vicinal hydroxyl groups to M1	4 coordinated	
$LnCl_3{\cdot}C_6H_{12}O_6{\cdot}9H_2O$	Pr-I, Nd-I	9	$P2_1/n$	2	O1 and O2 *cis* vicinal hydroxyl groups to M1	7 coordinated, 2 hydrogen-bonded	
$CsCl{\cdot}C_6H_{12}O_6$	Cs-I	10	$P2_1/n$	7	O1 and O2 to M1; O3 and O4 to M2; O5 and O6 to M3; O6 to M4		3
$LnCl_3{\cdot}C_5H_{10}O_5{\cdot}5H_2O$	Sm-R, Pr-R, La-R, Nd-R, Ce-R, Eu-R	9	$P2_1$	3	O1, O2 and O3 to M1 (α-pyranose $^4C_1$, β-pyranose $^1C_4$)	5 coordinated	1
$CaCl_2{\cdot}C_5H_{10}O_5{\cdot}3H_2O$	Ca-R	8	$P2_12_12_1$	5	O1, O2 and O3 to M1; O4 and O5 to M2 (furanose)	3 coordinated	
$CsCl{\cdot}C_5H_{10}O_5$	Cs-R	8	$P2_12_12_1$	5	O1 and O2 to M1, O4 and O5 to M2, O1 to M3		3

dx.doi.org/10.1021/ic402027j | *Inorg. Chem.* 2013, 52, 13132−13145

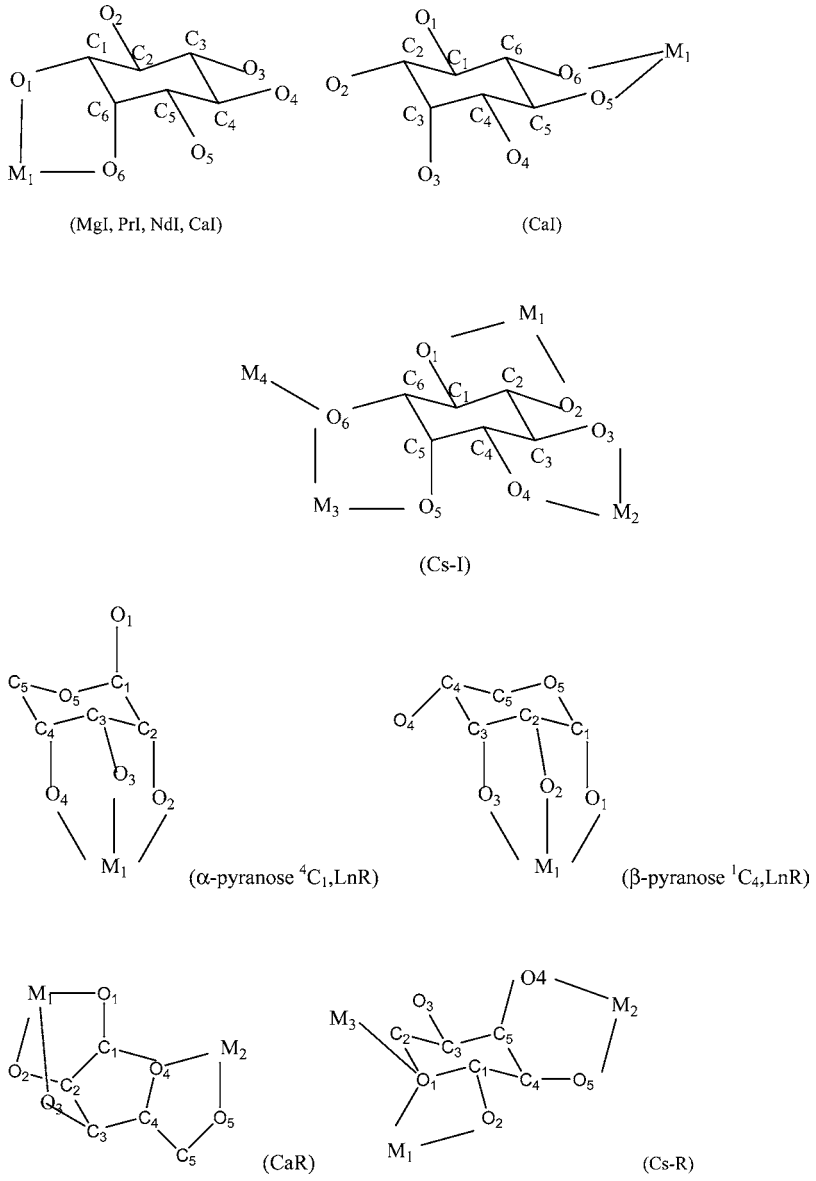

Figure 7. Coordination modes of D-ribose and *myo*-inositol with metal ions.

and Cl1#3−Cs1−Cl1−Cs1#3 are 180.0° and 0.0°, respectively, which indicates that Cl and Cs atoms are in a plane.

D-Ribose and *myo*-inositol have different coordination modes; they are coordinated to three to four cesium ions, to form complicated coordination structures. Chloride ions are coordinated to metal ions, and no water molecule exists in the two structures. The structures of cesium with D-ribose and *myo*-inositol are different with those with calcium and lanthanide ions. Cesium complexes with other ligands also can have structures different from those of other metal ions. For example, cesium chloride−cholic acid complex has a different coordination structure in comparison to other metal ions.[60]

FIR and THz Spectra of D-Ribose, Cesium Chloride−D-Ribose Complex, *myo*-Inositol, and Cesium Chloride−*myo*-Inositol Complex. FIR and THz are effective methods for determining the formation of metal−ligand complexes.[61−63] The FIR spectra of D-ribose and cesium chloride−D-ribose complex are shown in Figure 4. As shown in the figure, in the 650−50 cm^{-1} region the bands of Cs-R are located at 586, 534, 450, 405, 334, 283, 210, 175, 126, 108, and 68 cm^{-1}. After complexation with Cs ion, new bands are observed in comparison to those of D-ribose; most of them should be related to Cs−O and Cs−Cl vibrations. The bands near 200 cm^{-1} are usually assigned as M−O vibrations for metal−sugar complexes;[61] therefore, the bands at 283, 210, and 175 cm^{-1} belong to M−O vibrations and 126 and 108 cm^{-1} bands may be related to Cs−Cl vibrations. The bands may also be related to M−O−H, M−O−C, and O−M−O deformations or out of plane vibrations, etc. The peak positions and relative intensities of the bands in Cs-R are changed in comparison to those of D-ribose, which confirm the formation of metal complex.

The FIR spectra of *myo*-inositol and its cesium chloride complex also indicate the formation of the metal complex. The changes in peak positions and relative intensities are evident after complexation: for example, the bands in the 400−100 cm^{-1} region usually assigned to ν(M−O) and ν(M−Cl0 are shifted from 389, 370, 331, 300, 281, 216, 185, and 103 cm^{-1} to 392, 368, 344, 316, 290, 242, 209, 180, 156, 126, and 105 cm^{-1}, which reflect the changes of the conformation of *myo*-inositol and the formation of M−O and M−Cl bonds.

dx.doi.org/10.1021/ic402027j | *Inorg. Chem.* 2013, 52, 13132−13145

THz bands are mainly related to lattice vibrations, hydrogen bonds, etc.[64−67] The THz spectrum of cesium chloride−D-ribose complex is shown in Figure 5. The THz absorption bands are located at 1.43, 2.08, and 2.43 THz (48, 69, and 81 cm^{-1}) for Cs-R (1.11, 1.58, 1.93, 2.11, 2.28 THz (37, 53, 64, 70, 76 cm^{-1}) for D-ribose).[62] The strongest band is located at 69 cm^{-1} in the THz spectrum. This band position at 69 cm^{-1} is consistent with the corresponding peak (68 cm^{-1}) in its FIR spectrum. The FIR and THz spectra confirm the formation of the metal complex.

In the THz spectrum of cesium chloride−*myo*-inositol complex several bands exist, including bands at 1.29, 1.72, 1.90, and 2.17 THz (43, 57, 63, and 72 cm^{-1}). The THz absorption bands are located at 1.00, 1.46, 1.58, 1.82, and 2.05 THz (33, 49, 53, 61, and 68 cm^{-1}) for *myo*-inositol. The changes in band positions and relative intensities in the THz spectra indicate the formation of cesium chloride−*myo*-inositol complex.

Raman Spectra of the Cesium Chloride−D-Ribose and Cesium Chloride−*myo*-Inositol Complexes. The Raman spectra of D-ribose and its cesium chloride complex are shown in Figure 6. The intensities of ν(OH) are decreased in Raman spectra, and ν(CH) becomes stonger than ν(OH). The ν(OH) band of Cs-R is located at 3254 cm^{-1}. The ν(CH) bands are located in the 3000−2800 cm^{-1} region: 2983, 2921, and 2871 cm^{-1} for Cs-R. Many bands appear in the fingerprint region, which are related to ν(CO), ν(CC), δ(CCO), δ(COC), etc. $\delta(CH_2)$ is shifted from 1457 to 1453 cm^{-1}, $\omega(CH_2)$ is shifted from 1364 and 1322 cm^{-1} to 1360 and 1330 cm^{-1}, and $\tau(CH_2)$ is shifted from 1276 to 1275 cm^{-1} in Cs-R. ν(CO) bands at 1162 and 1121 cm^{-1} shift to 1153 and 1117 cm^{-1} after complexation. δ(COH) at 1061 cm^{-1} shifts to 1067 and 1052 cm^{-1} in Cs-R, which reflects the coordination of hydroxyl groups of D-ribose. ν(CC) at 887 cm^{-1} band shifts to 879 cm^{-1} after complexation. The bands at 805 and 730 cm^{-1} related to δ(CCO) are shifted to 795 and 733 cm^{-1}. The strongest band at 544 cm^{-1} in D-ribose is shifted to 539 cm^{-1} in Cs-R. These bands have different shifts in comparison to the spectrum of D-ribose, which also indicates the formation of cesium complex.

On comparison of the FTIR and Raman spectra of Cs-R, ν(OH) vibrations are strong in the IR spectrum but weak in the Raman spectrum and vice versa for the ν(CH) vibrations. In the 1500−650 cm^{-1} region, some peak positions are similar in the IR and Raman spectra, for example, 1153, 1118, 1052, 999, 880, 734, and 663 cm^{-1} in the IR spectrum and 1153, 1117, 1052, 1000, 879, 733, and 666 cm^{-1} in the Raman spectrum, but the relative intensities of the bands have large differences. The stronger bands are located at 1153, 1030, and 950 cm^{-1} in the IR spectrum of Cs-R, but the 879 cm^{-1} band is the strongest in this region in the Raman spectrum of Cs-R. This may be explained by the fact that IR is sensitive to vibrations of polar groups but Raman is mostly related to vibrations of nonpolar groups.

On comparison of the FIR and Raman spectra of Cs-R, the peak positions are similar to some extent: for example, the bands are located at 586, 534, 450, 405, 334, 283, 210, 175, 126, 108, and 68 cm^{-1} in the FIR spectrum and at 591, 539, 453, 403, 342, 312, 283, 199, 167, and 124 cm^{-1} in the Raman spectrum of Cs-R, which reflects the vibrations of the D-ribose ring, ν(M−O) and ν(M−Cl) vibrations, etc.

The Raman spectra of *myo*-inositol and cesium chloride−*myo*-inositol complex also indicate the formation of a metal complex. The weak ν(OH) bands are located at 3340 and 3238 cm^{-1} in Cs-I, and the ν(CH) vibrations are at 2919 and 2881 cm^{-1} (2959, 2922, 2885, and 2851 cm^{-1} for *myo*-inositol), which shows the changes in the CH chain. Many bands appear in the 1500−100 cm^{-1} region after complexation, which reflects the coordination of *myo*-inositol. The bands at 1356, 1325, 1279, and 1245 cm^{-1} mainly related to δ(COH), δ(CCH), and δ(CCO) are shifted to 1391, 1351, 1325, and 1254 cm^{-1} in Cs-I. The ν(CC) and ν(CO) vibrations mainly located at 1217, 1195, 1116, 1063, and 1007 cm^{-1} in *myo*-inositol are shifted to 1229, 1196, 1132, 1121, 1091, 1064, 1037, and 1011 cm^{-1} in Cs-I, and more bands appear after complexation, which shows the coordination of hydroxyl groups. The strong bands at 505 and 430 cm^{-1} in *myo*-inositol are shifted to 509 and 428 cm^{-1} in Cs-I. The bands in the 400−100 cm^{-1} region related to the ring deformation, ν(M−O), and ν(M−Cl) also shows the changes of band positions and relative intensities, which indicates the formation of the metal complex.

CONCLUSIONS

Cesium chloride−D-ribose and cesium chloride−*myo*-inositol complexes were obtained and characterized. For D-ribose, the single-crystal structure results show that the cesium ion has a structure different from those of calcium− and lanthanide−D-ribose complxes. Cs^+ is coordinated to O1 and O2 of one D-ribose molecule, O1 of the second D-ribose molecule, O4 and O5 of the third D-ribose molecule, and three chloride ions. The coordination number of the cesium ion is 8. The D-ribose molecule is in a pyranose form and provides O1 and O2 to one cesium ion, O1 also connected to another cesium ion, and O4 and O5 coordinated to the third cesium ion, respectively. O3 of D-ribose only forms hydrogen bonds. A new conformation of D-ribose was observed here. Cesium ion is connected to three chloride ions, and one chloride ion is also connected to three cesium ions. For *myo*-inositol, its cesium complex has a complicated structure: Cs^+ is 10-coordinated to three chloride ions, O1 and O2 from one *myo*-inositol molecule, O3 and O4 from another *myo*-inositol molecule, O5 and O6 from the third *myo*-inositol molecule, and O6 from the fourth *myo*-inositol molecule.

The various coordination modes of D-ribose and *myo*-inositol with different metal ions are shown in Table 4 and Figure 7, which indicate the complexity of the coordination structures of carbohydrate with metal ions. For D-ribose and *myo*-inositol complexes, Cs^+ has a high coordination number because of its large atom radius and no water, but chloride ion appears in the coordination sphere in the cesium complexes. FTIR results indicate the coordination of hydroxyl groups to cesium ion and changes in the conformation of the ligands and hydrogen bonds. FIR and THz spectra also confirm the formation of two cesium complexes. The changes in the Raman spectra of Cs−D-ribose and Cs−*myo*-inositol complexes are related to the rearrangement of the CH chain, the variation of conformation of D-ribose and *myo*-inositol, and the formation of a Cs complex. Crystal structures and FTIR, FIR, THz, and Raman spectra provide detailed information on the structure and coordination of hydroxyl groups to metal ions in the cesium chloride−D-ribose and cesium chloride−*myo*-inositol complexes. The results also indicate that for compounds which are surely coordination compounds but which cannot form a single crystal for the X-ray analysis, IR, Raman, FIR, and THz spectra may be effective methods to deduce unknown structures.

ASSOCIATED CONTENT

Supporting Information

Crystallographic data in CIF format for these lanthanide-erythritol complexes and a table giving C−O and C−C distances and bond angles of *myo*-inositol and its metal

dx.doi.org/10.1021/ic402027j | Inorg. Chem. 2013, 52, 13132−13145

complexes. This material is available free of charge via the Internet at http://pubs.acs.org.

AUTHOR INFORMATION

Corresponding Authors

*L.Y.: tel, 86-10-62751889; fax, 86-10-62758849; e-mail, yanglm@pku.edu.cn.

*Y.X.: e-mail, xyz@pku.edu.cn.

Notes

The authors declare no competing financial interest.

ACKNOWLEDGMENTS

Financial support from the National Natural Science Foundation of China (grants 21001009 and 50973003), the State Key Project for Fundamental Research of MOST (2011CB808304), and the National High-tech R&D Program of China (863 Program) of MOST (2010AA03A406) and the Scientific Research Project of Beijing Municipal Commission of Education and Beijing Natural Science Foundation (Grant No. KZ201310028032) are gratefully acknowledged. We thank Prof. Xiang Hao, Tongling Liang, and Lin Wang (Institute of Chemistry, Chinese Academy of Sciences) and Prof. Jian Hao (Beijing University of Chemical Technology) for invaluable assistance with the X-ray crystallography.

REFERENCES

(1) Gyurcsik, B.; Nagy, L. *Coord. Chem. Rev.* **2000**, *203*, 81−148.

(2) Hartinger, C. G.; Nazarov, A. A.; Ashraf, S. M.; Dyson, P. J.; Keppler, B. K. *Curr. Med. Chem.* **2008**, *15*, 2574−2591.

(3) Vetter, C.; Pornsuriyasak, P.; Schmidt, J.; Rath, N. P.; Ruffer, T.; Demchenko, A. V.; Steinborn, D. *Dalton Trans.* **2010**, *39*, 6327−6338.

(4) Li, G. H.; Badkar, A.; Kalluri, H.; Banga, A. K. *J. Pharm. Sci.* **2010**, *99*, 1931−1941.

(5) Storr, T.; Merkel, M.; Song-Zhao, G. X.; Scott, L. E.; Green, D. E.; Bowen, M. L.; Thompson, K. H.; Patrick, B. O.; Schugar, H. J.; Orvig, C. *J. Am. Chem. Soc.* **2007**, *129*, 7453−7463.

(6) Taccardi, N.; Assenbaum, D.; Berger, M. E. M.; Bosmann, A.; Enzenberger, F.; Wolfel, R.; Neuendorf, S.; Goeke, V.; Schodel, N.; Maass, H.-J.; Kistenmacher, H.; Wasserscheid, P. *Green Chem.* **2010**, *12*, 1150−1156.

(7) Gottschaldt, M.; Schubert, U. S. *Chem. Eur. J.* **2009**, *15*, 1548−1557.

(8) Garcia, I.; Marradi, M.; Penades, S. *Nanomedicine* **2010**, *5*, 777−792.

(9) Alvarez, A. M.; Moreldesrosiers, N.; Morel, J. P. *Can. J. Chem.* **1987**, *65*, 2656−2660.

(10) Chen, Z. G.; Moreldesrosiers, N.; Morel, J. P.; Detellier, C. *Can. J. Chem.* **1994**, *72*, 1753 −1757.

(11) Moreldesrosiers, N.; Lhermet, C.; Morel, J. P. *J. Chem. Soc., Faraday Trans.* **1993**, *89*, 1223−1228.

(12) Araki, K.; Shiraishi, S. *Carbohydr. Res.* **1986**, *148*, 121−126.

(13) Lenkinski, R. E.; Reuben, J. *J. Am. Chem. Soc.* **1976**, *98* (11), 3089−3094.

(14) Ortiz, P.; Fernandez-Bertran, J.; Reguera, E. *Spectrochim. Acta, Part A* **2005**, *61* (8), 1977−1983.

(15) Petrou, A. L. *Coord. Chem. Rev.* **2002**, *228*, 153−162.

(16) Banipal, P. K.; Singh, V.; Banipal, T. S. *J. Chem. Thermodyn.* **2010**, *42*, 90−103.

(17) Yang, E.; Zhou, L. X.; Zhang, Y. F. *Acta Phys.-Chim. Sin.* **2002**, *18* (3), 253−259.

(18) Angyal, S. J.; Greeves, D.; Pickles, V. A. *J. Chem. Soc., Chem. Commun.* **1974**, *15*, 589−590.

(19) Angyal, S. J.; Hickman, R. J. *Aust. J. Chem.* **1975**, *28*, 1279−1287.

(20) Zhao, Q.; Xing, S. K.; Zhang, Q.; Sun, D. Z. *Acta Phys.-Chim. Sin.* **2008**, *24* (5), 890−894.

(21) Sun, D. Z.; Zheng, W. Q.; Qu, X. K.; Li, L. *J. Chem. Eng. Data* **2007**, *52*, 898−901.

(22) Zhao, Q.; Sun, Z. J.; Zhang, Q.; Xing, S. K.; Liu, M.; Sun, D. Z.; Li, L. W. *Thermochim. Acta* **2009**, *487*, 1−7.

(23) Joshi, S. A.; Kulkarni, N. D. *Chem. Commun.* **2009**, *17*, 2341−2343.

(24) Guo, J. Y.; Lu, Y. *J. Carbohydr. Chem.* **2010**, *29*, 10−19.

(25) Lu, Y.; Guo, J. Y. *Carbohydr. Res.* **2006**, *341* (5), 610−615.

(26) Lu, Y.; Guo, J. Y. *Carbohydr. Res.* **2006**, *341* (5), 683−687.

(27) Lu, Y.; Deng, G. C.; Miao, F. M.; Li, Z. M. *Carbohydr. Res.* **2004**, *339* (10), 1689−1696.

(28) Lu, Y.; Deng, G. C.; Miao, F. M.; Li, Z. M. *Carbohydr. Res.* **2003**, *338* (24), 2913−2919.

(29) Lu, Y.; Deng, G. C.; Miao, F. M.; Li, Z. M. *J. Inorg. Biochem.* **2003**, *96* (4), 487−492.

(30) Su, Y. L.; Yang, L. M.; Weng, S. F.; Wu, J. G. *J. Rare Earths* **2002**, *20* (5), 339−342.

(31) Yang, L. M.; Wu, J. G.; Weng, S. F.; Jin, X. L. *J. Mol. Struct.* **2002**, *612* (1), 49−57.

(32) Yang, L. M.; Zhao, Y.; Xu, Y. Z.; Jin, X. L.; Weng, S. F.; Tian, W.; Wu, J. G.; Xu, G. X. *Carbohydr. Res.* **2001**, *334* (2), 91−95.

(33) Klufers, P.; Kunte, T. *Chem. Eur. J.* **2003**, *9*, 2013−2018.

(34) Mukhopadhyay, A.; Kolehmainen, E.; Rao, C. P. *Carbohydr. Res.* **2000**, *328*, 103−113.

(35) Bandwar, R. P.; Sastry, M. D.; Kadam, R. M.; Rao, C. P. *Carbohydr. Res.* **1997**, *297*, 333−339.

(36) Wood, R. A.; James, U. J.; Angyal, S. J. *Acta Crystallogr., Sect. B* **1977**, *33*, 2248−2251.

(37) Yang, L. M.; Tao, D. L.; Sun, Y.; Jin, X. L.; Zhao, Y.; Yang, Z. L.; Weng, S. F.; Wu, J. G.; Xu, G. X. *J. Mol. Struct.* **2001**, *560*, 105−113.

(38) Yang, L. M.; Wang, Z. M.; Zhao, Y.; Tian, W.; Xu, Y. Z.; Weng, S. F.; Wu, J. G. *Carbohydr. Res.* **2000**, *329*, 847−853.

(39) Cook, W. J.; Bugg, C. E. *Acta Crystallogr., Sect. B* **1973**, *29*, 2404−2411.

(40) Blank, G. *Acta Crystallogr., Sect. B* **1973**, *29*, 1677−1683.

(41) Morgenstern, B.; Kutzky, B.; Neis, C.; Stucky, S.; Hegetschweiler, K.; Garribba, E.; Micera, G. *Inorg. Chem.* **2007**, *46*, 3903−3915.

(42) Hegetschweiler, K.; Hausherr-Primo, L.; Koppenol, W. H.; Gramlich, V.; Odier, L.; Meyer, W.; Winkler, H.; Trautwein, A. X. *Angew. Chem., Int. Ed. Engl.* **1995**, *34*, 2242−2243.

(43) Bugg, C. E.; Cook, W. J. *J. Chem. Soc., Chem. Commun.* **1972**, *12*, 727−729.

(44) Dheu-Andries, M. L.; Perez, S. *Carbohydr. Res.* **1983**, *124*, 324−332.

(45) Cook, W. J.; Bugg, C. E. In *Metal-Ligand Interactions in Organic Chemistry and Biochemistry*; Pullman, B., Goldblum, N., , Eds.; Springer: Berlin, 1977; Part 2, pp 231−256.

(46) Einspahr, H.; Bugg, C. E. In *Calcium and its Role in Biology*; SigelH., Sigel, A., Eds.; Mareel Dekker: New York, 1984; Metal iIons in Biological Systems *17*, pp 51−97.

(47) Yang, L. M.; Su, Y. L.; Xu, Y. Z.; Wang, Z. M.; Guo, Z. H.; Weng, S. F.; Yan, C. H.; Zhang, S. W.; Wu, J. G. *Inorg. Chem.* **2003**, *42*, 5844−5856.

(48) Yang, L. M.; Hua, X. H.; Xue, J. H.; Pan, Q. H.; Yu, L.; Li, W. H.; Xu, Y. Z.; Zhao, G. Z.; Liu, L. M.; Liu, K. X.; Chen, J. E.; Wu, J. G. *Inorg. Chem.* **2012**, *51*, 499−510.

(49) Su, Y. L.; Yang, L. M.; Xu, Y. Z.; Wang, Z. M.; Weng, S. F.; Yan, C. H.; Wang, D. J.; Wu, J. G. *Inorg. Chem.* **2007**, *46*, 5508−5517.

(50) Angyal, S. J.; Craig, D. C. *Carbohydr. Res.* **1993**, *241*, 1−8.

(51) Accorsi, C. A.; Bertolasi, V.; Ferretti, V.; Gilli, G. *Carbohydr. Res.* **1989**, *191*, 91−104.

(52) Accorsi, C. A.; Bellucci, F.; Bertolasi, V.; Ferretti, V.; Gilli, G. *Carbohydr. Res.* **1989**, *191*, 105−116.

(53) Peralta-Inga, Z.; Johnson, G. P.; Dowd, M. K.; Rendleman, J. A.; Stevens, E. D.; French, A. D. *Carbohydr. Res.* **2002**, *337*, 851−861.

(54) Sheldrick, G. M. *Acta Crystallogr., Sect. A: Found. Crystallogr.* **2008**, *64*, 112−122.

(55) Hu, Y.; Wang, X. H.; Guo, L. T.; Zhang, C. L.; Liu, H. B.; Zhang, X. C. *Acta Phys. Sin.* **2005**, *54*, 4124−4128.
(56) Mathlouthi, M.; Seuvre, A. M.; Koenig, J. L. *Carbohydr. Res.* **1983**, *122*, 31−47.
(57) Wu, J. G. *Modern Fourier Transform Spectroscopic Techniques and Its Applications*; Science and Technology References Press: Beijing, 1994.
(58) Weng, S. F. *Fourier Transform Infrared Spectrometer*; Chemical Industry Press: Beijing, 2005; pp 270−272.
(59) Mathlouthi, M.; Koenig, J. L. *Adv. Carbohydr. Chem. Biochem.* **1986**, *44*, 7−89.
(60) Sun, Y.; Soloway, R. D.; Han, Y. Z.; Yang, G. D.; Wang, X. Z.; Liu, Z. J.; Yang, Z. L.; Xu, Y. Z.; Wu, J. G. *Steroids* **2002**, *67* (5), 385−392.
(61) Yang, L. Q.; Wu, J. G.; Zhou, Q.; Bian, J.; Yang, Y. M.; Xu, D. F.; Xu, G. X. *Mikrochim. Acta* **1997**, *14*, 251−252.
(62) Yang, L. M.; Sun, H. Q.; Weng, S. F.; Zhao, K.; Zhang, L. L.; Zhao, G. Z.; Wang, Y. G.; Xu, Y. Z.; Lu, X. Y.; Zhang, C. L.; Wu, J. G.; Chen, J. E. *Spectrochim. Acta, Part A* **2008**, *69*, 160−166.
(63) Yang, L. M.; Zhao, G. Z.; Li, W. H.; Liu, Y. F.; Shi, X. X.; Jia, X. F.; Zhao, K.; Lu, X. Y.; Xu, Y. Z.; Xie, D. T.; Wu, J. G.; Chen, J. E. *Spectrochim. Acta, Part A* **2009**, *73*, 884−891.
(64) Falconer, R. J.; Markelz, A. G. *J. Infrared, Millimeter, Terahertz Waves* **2012**, *33*, 973−988.
(65) Mclntosh, A. I.; Yang, B.; Goldup, S. M.; Watkinson, M.; Donnan, R. S. *Chem. Soc. Rev.* **2012**, *41*, 2072−2082.
(66) Theuer, M.; Harsha, S. S.; Molter, D.; Torosyan, G.; Beigang, R. *Chem. Phys. Chem.* **2011**, *12* (15), 2695−2705.
(67) Tan, P.; Huang, J.; Liu, K. F.; Xiong, Y. Q.; Fan, M. W. *Sci. China Inf. Sci.* **2012**, *55*, 1−15.